Materials Science in Semiconductor Processing 162 (2023) 107528

Contents lists available at ScienceDirect

Materials Science in Semiconductor Processing

journal homepage: www.elsevier.com/locate/mssp

Enhanced thermoelectricity in Bi-sprayed bismuth sulphide particles

Rafiq Mulla [a,*], Sajad Kiani [a], Alvin Orbaek White [a], Charles W. Dunnill [a], Andrew R. Barron [a,b,c,d,**]

[a] Energy Safety Research Institute, Swansea University, Bay Campus, Fabian Way, Swansea, SA1 8EN, UK
[b] Arizona Institute for Resilient Environments and Societies (AIRES), University of Arizona, Tucson, AZ, 85721, USA
[c] Department of Chemistry and Department of Materials Science and Nanoengineering, Rice University, Houston, TX, 77005, USA
[d] Faculty of Engineering, Universiti Teknologi Brunei, Brunei Darussalam

ARTICLE INFO

Keywords:
Thermoelectric
Bismuth sulphide
Doping
Composites
Electrical properties

ABSTRACT

Bismuth sulphide (Bi_2S_3), an n-type semiconductor that critically demonstrates the Seebeck effect with Seebeck coefficients of about 300 μVK^{-1}. However, its poor electrical conductivity makes it unsuitable for thermoelectric applications. In this study, we present a facile preparation method for fabricating Bi-sprayed Bi_2S_3 particles that alters their thermoelectric properties. Samples were created with differing Bi concentrations into the Bi_2S_3 compound to test for enhanced thermoelectric properties of the resulting Bi/Bi_2S_3 composites. The incorporation of excess Bi into Bi_2S_3 significantly improves the compound's electrical conductivity and optimises overall thermoelectric performance. The electrical conductivity of the Bi/Bi_2S_3 composites improved from 6.5 Scm^{-1} (for pristine Bi_2S_3) to 154 Scm^{-1} (for highest Bi added Bi_2S_3). Although the Seebeck coefficient of samples decreased with Bi incorporation, a high power factor (~390 $\mu Wm^{-1}K^{-2}$) has been achieved for an optimised composition of the composite. Incorporation of metallic Bi has led to an increase in the thermal conductivity of the samples, but the increase is not significant for the optimised composition of the composites where a high thermoelectric performance has been observed. Therefore, enhanced power factor and moderate thermal conductivity have resulted in a peak ZT value of 0.11 at room temperature. The strategy proposed here improves the thermoelectricity in Bi_2S_3 and shows excellent potential for developing better-performing thermoelectric compounds with excess elemental contents.

1. Introduction

Thermoelectric materials, which can produce electricity from heat, could play a promising role in a sustainable energy solution [1]. After years of research, Bi_2Te_3, PbTe, SnSe, Cu_2Se, Cu_2S, half-Heuslers, oxides, organic composites, have been found to have excellent thermoelectric properties [2–4]. A long-standing challenge to the widespread use of thermoelectric generators is finding high-performance materials from abundant and low-cost elements [5–12]. The conversion efficiency of a thermoelectric material is governed by its dimensionless figure of merit (ZT), defined as [13,14],

$$ZT = \frac{\alpha^2 \sigma T}{\kappa} \tag{1}$$

where α, σ, κ, and T are the Seebeck coefficient, the electrical conductivity, the total thermal conductivity, and the absolute temperature, respectively [13,15].

Many recent advances in improving the ZT of materials are linked to nanoscale phenomena and complex crystal structure formation [16–18]. New materials have now evolved into studies on bulk samples that contain nanostructured constituents or impurity particles prepared by chemical or physical methods at high temperatures [16,19]. The commercially available thermoelectric devices are mainly made with Bi_2Te_3, PbTe, and alloy compounds [20,21]. However, the scarcity of tellurium (Te) limits the use of such devices [15,22,23]. Recently, sulphur (S) and selenide (Se) based metal chalcogenides have received increased interest as non-tellurium candidates [24–29]. Among different metal chalcogenides, Bismuth sulphide (Bi_2S_3) has also been a candidate of interest on which research is focused to improve its thermoelectric performance [30–32]. However, the high electrical resistivity is one of the significant issues associated with the Bi_2S_3. In a recent study by Ge

* Corresponding author.
** Corresponding author. Energy Safety Research Institute, Swansea University, Bay Campus, Fabian Way, Swansea, SA1 8EN, UK.
E-mail addresses: rafiq.mulla@swansea.ac.uk (R. Mulla), a.r.barron@swansea.ac.uk (A.R. Barron).

https://doi.org/10.1016/j.mssp.2023.107528
Received 1 March 2023; Received in revised form 10 April 2023; Accepted 12 April 2023
Available online 15 April 2023

et al. Bi_2S_3@Bi core-shell nanowires were prepared by a hydrothermal method to enhance the thermoelectric properties of Bi_2S_3 [30]. Numerous efforts have also reported on improving its thermoelectric properties, such as element doping, micro and nanostructure design, texturing, etc [33–37]. The reported ZT values of Bi_2S_3-based composites fall within the range of 0.05–0.50 in the temperature range of 300 K–650 K [30,32].

Herein, we report a preparation method for Bi-sprayed Bi_2S_3 particles to fabricate Bi/Bi_2S_3 bulk composite to investigate their thermoelectric changes. The fabrication process is a single step, straightforward methodology involving facile sputter deposition of Bi onto Bi_2S_3 particles. The resulting Bi/Bi_2S_3 composites have shown exciting results with enhanced electrical conductivity and thermoelectric power factor ($\alpha^2\sigma$), implying that Bi_2S_3 can be a promising thermoelectric material after suitable modifications in its elemental compositions.

2. Experimental details

2.1. Synthesis procedure

Bismuth (99.9% purity) sputter target and bismuth sulphide (Bi_2S_3) powder were used as primary sources and were obtained from PI-KEM Ltd. And Alfa Aesar, respectively. In a typical process, Bi was deposited by sputter-coating (Model: Quorum Q150T-S coater) onto Bi_2S_3 powder particles that were evenly spread in a Petri dish (6 mm dia.). A series of Bi/Bi_2S_3 composite samples were obtained by different levels of Bi deposition (thickness: 20 nm–500 nm, deposition rate: ~20 nm min^{-1}) at room temperature under argon atmosphere. The as-obtained Bi-coated Bi_2S_3 powder was then finely ground with a pestle mortar to form uniform mixing of the particles to obtain a Bi/Bi_2S_3 composite. Bulk solid pellets of 16 mm diameter were prepared using a 12 tonne press with a pressing time of 20 min at room temperature.

2.2. Material characterisation

The surface morphology of pristine Bi_2S_3 and Bi/Bi_2S_3 composite samples was determined by field emission scanning electron microscopy (FESEM) using a Hitachi TM3030 SEM. The chemical characteristics of the samples were obtained using an Oxford X-map energy dispersive X-ray spectrometer (EDX) system. The phase structures of composites were measured by powder X-ray diffraction (XRD) using a Bruker D8 Discover diffractometer with Cu K_α radiation.

The Seebeck coefficient (α) of the disk-shaped samples, which were cut into bars, was measured using a lab-built setup [38,39]. In a typical measurement, the voltage developed (ΔV) and temperature difference (ΔT) between the hot and the cold sides of the samples were used to estimate the Seebeck coefficient (α) using the expression [38],

$$\alpha = -\left(\frac{\Delta V}{\Delta T}\right) \quad (2)$$

Temperature differences of 2–5 °C were applied along the samples, and multiple readings were recorded to confirm reproducibility of the results and average values have been used to plot the data. The electrical conductivity of the samples was obtained by a standard four-probe method. The samples' thermoelectric power factors (PF) were calculated from the Seebeck coefficient and the electrical conductivity determine using a standard equation, $PF = \alpha^2\sigma$.The thermal conductivities of the samples were measured by a steady state method, according to the parallel thermal conductance technique using a lab-built measurement systemin a vacuum (10^{-4} mbar) [40]. The carrier concentration and mobility of the samples were measured at room temperature using a physical properties measurement system.

3. Results and discussion

Fig. 1 shows the XRD patterns of pure Bi_2S_3 (S1) and Bi_2S_3 samples with varying levels of excess Bi incorporation (with Bi spray thickness x = 20 nm (S2), 50 nm (S3), 100 nm (S4), 200 nm (S5), 300 nm (S6), 500 nm (S7)). The XRD peaks closely resembled the orthorhombic structure of Bi_2S_3 with a standard pattern card (PDF#17–0320) with additional minor peaks of Bi.

Fig. 2 shows the SEM images of the Bi_2S_3 and Bi-coated Bi_2S_3 samples. All samples show varying particle sizes in the range of a few microns, and there are no visible changes in the particles after Bi coating. The EDS mapping was performed to study the changes in the Bi and S ratio in the samples; the results are in Fig. 2 (e and f). The as-received Bi_2S_3 compound had an elemental (at%) ratio of 41.9:59.1 (Bi:S), which is in near agreement with the standard atomic ratio of Bi_2S_3 (Bi:S – 2:3). Incorporating Bi increased the Bi content of the samples with ratios of Bi:S (at%) – 44.2:55.8 for S3, 46.5:53.5 for S5, 48.4:51.6 for S7. The increased Bi content indicates a successful incorporation of Bi with different concentrations. The Bi-coated particles are uniformly distributed across the entire sample after a thorough grinding of each sample after the Bi deposition process, as it can be seen from the EDS elemental mapping images provided in the *Supplementary Information* of the paper (Fig. S1).

All the thermoelectric measurements are displayed in Fig. 3. As shown in Fig. 3a and b, the difference between the Seebeck coefficient (α) and electrical conductivity (σ) of the starting compound Bi_2S_3 and Bi-coated Bi_2S_3 (samples-S7) was found to be quite large. Starting Bi_2S_3 compound has a very large α of ~350 μVK^{-1}, whereas sample S7 exhibits a very low S of ~130 μVK^{-1}. With the incorporation of Bi,

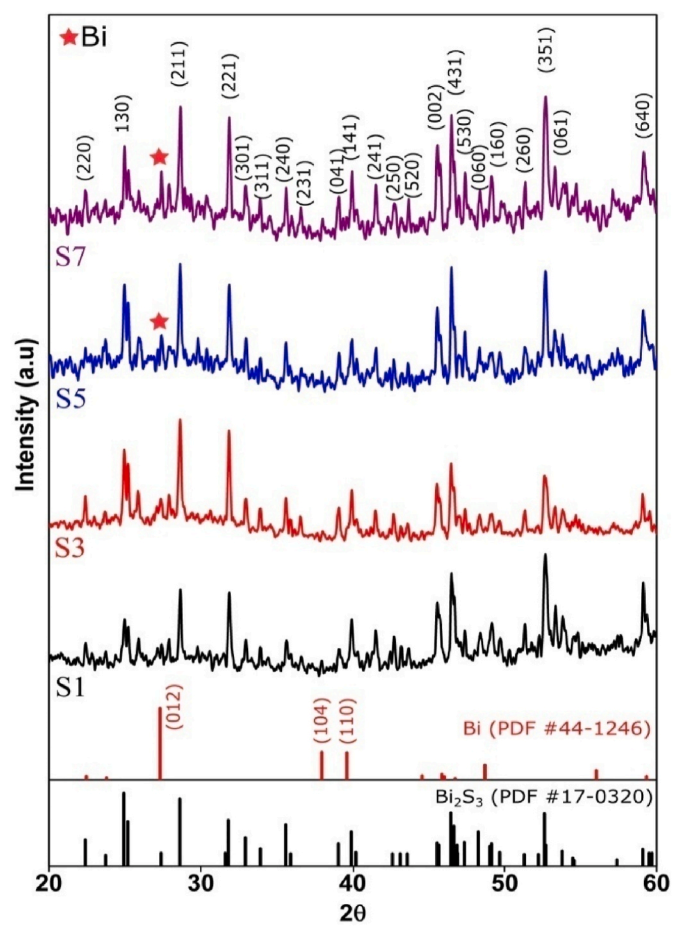

Fig. 1. XRD patterns of pristine Bi_2S_3 (S1) and Bi/Bi_2S_3 composites with different levels Bi incorporation (S3, S5, S7).

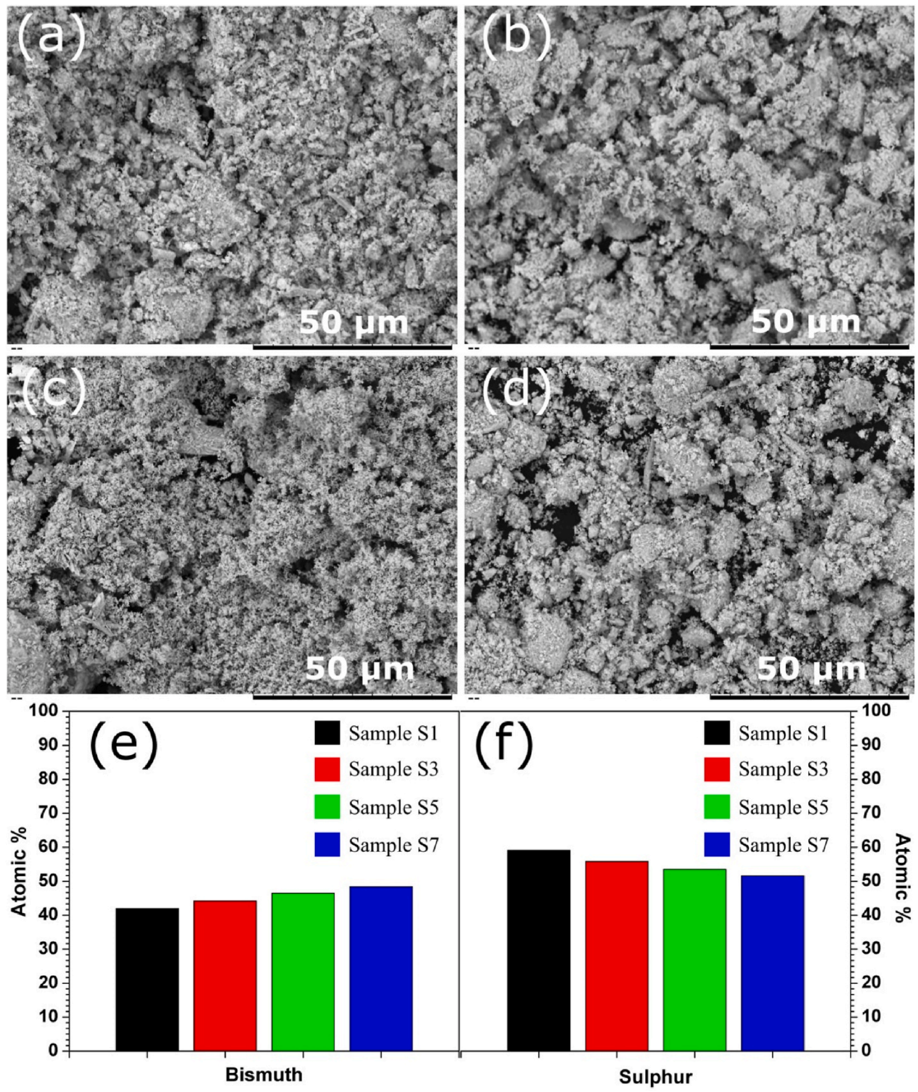

Fig. 2. SEM images of the Bi_2S_3 particles added with different levels of Bi coating: (a) S1, (b) S3, (c) S5, (d) S7. Figures (e) and (f) are the elemental (Bi and S) scanning results acquired from the samples.

initially, to create Bi/Bi_2S_3 composites with small quantities of Bi, no notable changes were observed in the α and σ values. However, after sample S3, there was a significant increase in the electrical conductivity (σ), mostly dominated by metallic Bi properties. In contrast, the α of Bi/Bi_2S_3 compound decreased with the increase of Bi content. The observed σ of the highest Bi-incorporated sample (sample-S7) is 154 Scm^{-1} but only 6.5 Scm^{-1} for pristine Bi_2S_3 (sample-S1). Although the α of sample-S1 and sample-S7 differ widely, the decrease in α is slight with the increase of Bi content for the Bi/Bi_2S_3 composite compounds, which is a beneficial factor. As a result, the power factor (PF) has improved in the case of most composites (from sample-S4 to S7) and reached a maximum value of ~390 $\mu Wm^{-1}K^{-2}$ for the sample-S6 composite. Fig. 3d displays the excess Bi dependence of the total thermal conductivity (κ) of the Bi/Bi_2S_3 composites. The κ values of all the composites are not much affected for initial compositions (until sample-S4) but slightly higher than that of pristine Bi_2S_3 in sample-S5, S6, and S7. Such an increase in the κ of the Bi/Bi_2S_3 composites (S5, S6, and S7) indicates the role of metallic Bi on the composites' thermal properties. Simultaneously, enhanced PF and moderate κ have resulted in a peak ZT value of 0.11 at room temperature for sample-S6 composite (Fig. 3e). The temperature dependence of α, σ, and PF were measured from room temperature to 120 °C (Fig. 4). The Seebeck coefficient, as shown in Fig. 5a, increasing the temperature up to 120 °C had a small decreasing effect on this value. The temperature dependence on electrical conductivity had a negligible effect on the measured temperature range (Fig. 4b). The resultant power factor values (Fig. 4c) of one of the best-performing samples (sample-S6) exhibit values ranging from 350 to 430 $\mu Wm^{-1}K^{-2}$.

Furthermore, the data on the carrier concentration and mobility of Bi/Bi_2S_3 samples shown in Fig. 5a confirm that the Bi layers on Bi_2S_3 particles act as conducting paths for charge carriers, resulting in increased mobility of the samples with Bi addition. The increased Bi content in the compound has also raised the carrier concentration, leading to an increase in the compound's σ. It is important to note that, despite a significant enhancement in the σ of the samples, there has been only a slight increase in κ. It is believed that the presence of interfaces between Bi_2S_3 and Bi plays a major role in controlling phonons, thus overcoming the detrimental effects of κ through the enhancements in σ.

Such a moderate κ and optimised α of composites indicates enhanced phonon and charge carrier scattering at the interfaces [41]. Nonetheless, the overall thermoelectric ZT of the composites has improved. The interfaces created between Bi and Bi_2S_3 and/or possible accommodation of Bi layers between the Bi_2S_3 grains in the bulk samples help scatter phonons as well as help maintain high Seebeck coefficients [41]. Such interfacial structures have resulted in overall improvements in thermoelectric properties. Previous studies on interface effects of different thermoelectric materials suggest that energy barrier scattering can help

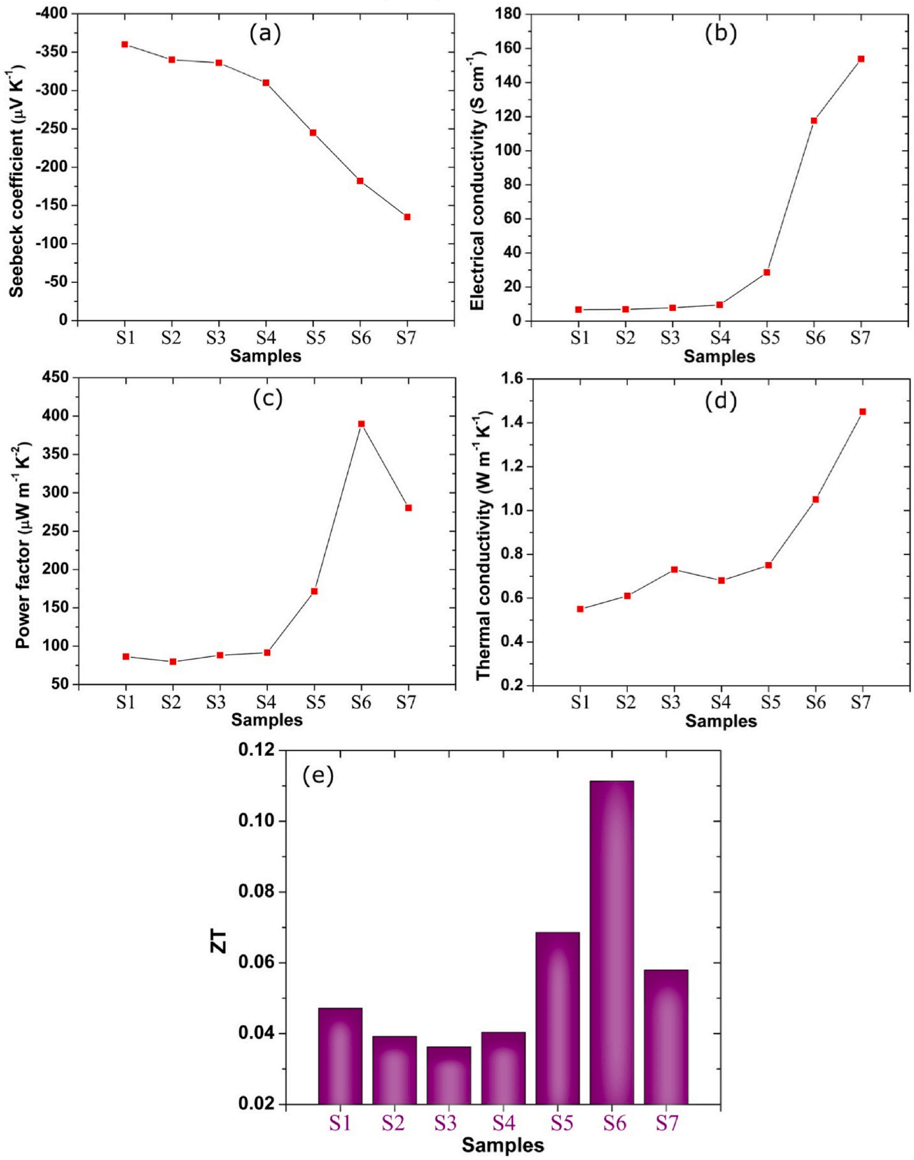

Fig. 3. Room temperature Seebeck coefficient (a), electrical conductivity (b), power factor (c), thermal conductivity (d), and ZT values (e) of the Bi/Bi_2S_3 samples.

achieve high power factors and decouple thermal and electrical transport phenomena [42,43]. Thus, our results reveal the enhanced potential of Bi/Bi_2S_3 composites for thermoelectric applications compared to the pristine Bi_2S_3 compound.

4. Conclusion

The current study has demonstrated a straightforward method for producing Bi/Bi_2S_3 composites with great potential for thermoelectric applications. By coating Bi layers onto Bi_2S_3 particles in the composites, both the power factors and the thermoelectric figure of merit (ZT) have been simultaneously increased. The slight increase in thermal conductivity suggests that the interfaces between Bi and Bi_2S_3, as well as the accommodation of Bi layers within the bulk Bi_2S_3 samples, can effectively scatter phonons and maintain high Seebeck coefficients. Overall, these unique composite structures have led to significant improvements in thermoelectric properties.

While the performance of the Bi/Bi_2S_3 composite presented here is relatively lower than that of well-established Bi_2Te_3 compounds, this tellurium-free compound with low-cost and abundant sulphur as a replacement for tellurium has the potential to be a promising material for future thermoelectric applications. However, detailed research is necessary to optimize the thermoelectric performance of Bi_2S_3. Nonetheless, given the scarcity of other additive materials like Te, the simple and facile addition of Bi to Bi_2S_3 composites offers a unique and cost-effective pathway for producing enhanced thermoelectric materials.

CRediT authorship contribution statement

Rafiq Mulla: Writing – original draft, Visualization, Validation, Methodology, Investigation, Formal analysis, Conceptualization. **Sajad Kiani:** Writing – review & editing, Investigation, Formal analysis. **Alvin Orbaek White:** Writing – review & editing, Supervision. **Charles W. Dunnill:** Writing – review & editing, Supervision. **Andrew R. Barron:** Writing – review & editing, Supervision, Resources, Project administration, Funding acquisition.

Declaration of competing interest

The authors declare that they have no known competing financial interests or personal relationships that could have appeared to influence the work reported in this paper.

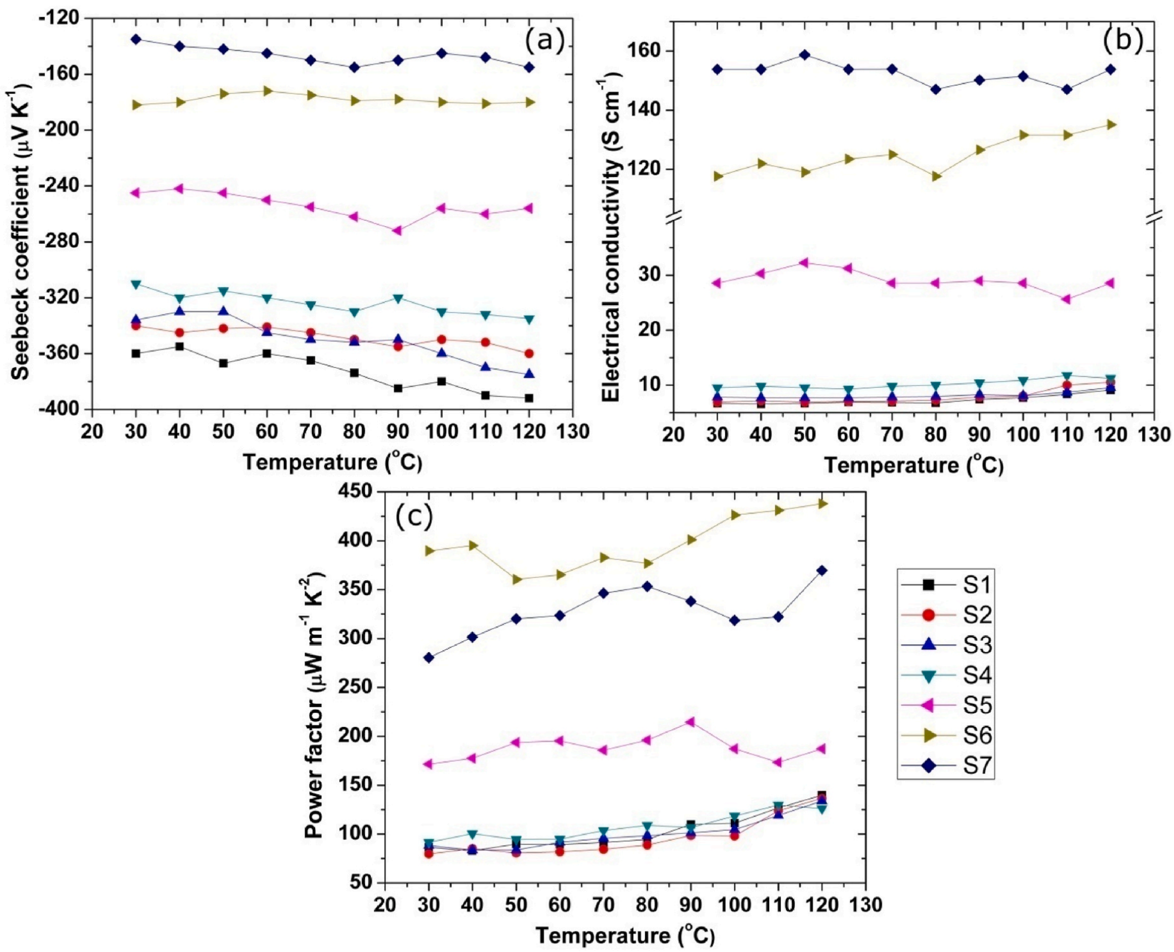

Fig. 4. Measured variations in the (a) Seebeck coefficient, (b) electrical conductivity, and (c) power factors of the Bi/Bi_2S_3 composites.

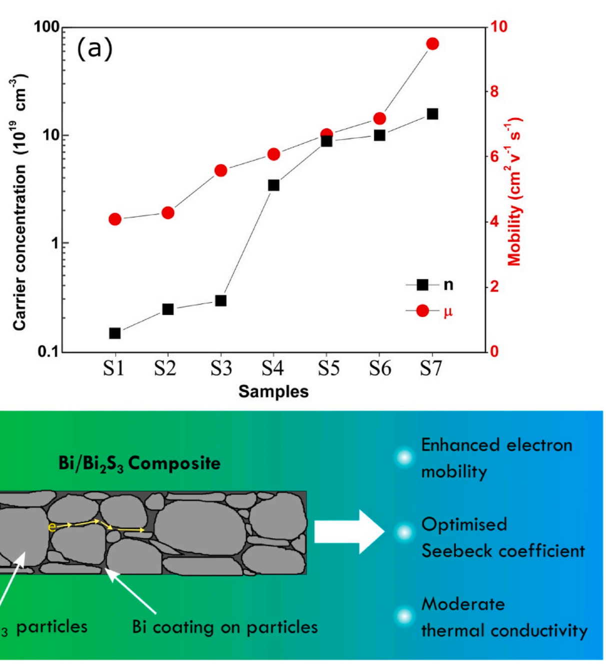

Fig. 5. (a) Carrier concentration (n) and mobility (μ) of Bi/Bi_2S_3 samples (at room temperature), and (b) a schematic that illustrates the Bi/Bi_2S_3 solid composite's conducting paths for better charge mobility and interfaces that help optimize the overall thermoelectric performance of the composites.

Data availability

Data will be made available on request.

Acknowledgments

Authors are thankful to the Welsh Government (EU European Regional Development Fund) for funding the RICE (Reducing Industrial Carbon Emission) project (Grant Number: 81435), and for funding AOW as Sêr Cymru II Fellow and Welsh Government Capital Fund (Grant number: 290).

Appendix A. Supplementary data

Supplementary data to this article can be found online at https://doi.org/10.1016/j.mssp.2023.107528.

References

[1] G.J. Snyder, E.S. Toberer, Complex thermoelectric materials, Nat. Mater. 7 (2008) 105.

[2] J. Wei, L. Yang, Z. Ma, P. Song, M. Zhang, J. Ma, F. Yang, X. Wang, Review of current high-ZT thermoelectric materials, J. Mater. Sci. 55 (27) (2020) 12642–12704.

[3] J. Zhou, Y. Wu, Z. Chen, P. Nan, B. Ge, W. Li, Y. Pei, Manipulation of defects for high-performance thermoelectric PbTe-based alloys, Small Structures 2 (7) (2021), 2100016.

[4] L.-D. Zhao, S.-H. Lo, Y. Zhang, H. Sun, G. Tan, C. Uher, C. Wolverton, V.P. Dravid, M.G. Kanatzidis, Ultralow thermal conductivity and high thermoelectric figure of merit in SnSe crystals, Nature 508 (2014) 373.

[5] S. Aminorroaya Yamini, H. Wang, Z.M. Gibbs, Y. Pei, D.R.G. Mitchell, S.X. Dou, G. J. Snyder, Thermoelectric performance of tellurium-reduced quaternary p-type lead–chalcogenide composites, Acta Mater. 80 (2014) 365–372.

[6] O. Caballero-Calero, J.R. Ares, M. Martín-González, Environmentally friendly thermoelectric materials: high performance from inorganic components with low toxicity and abundance in the earth, Advanced Sustainable Systems 5 (11) (2021), 2100095.

[7] E. Isotta, J. Andrade-Arvizu, U. Syafiq, A. Jiménez-Arguijo, A. Navarro-Güell, M. Guc, E. Saucedo, P. Scardi, Towards low cost and sustainable thin film thermoelectric devices based on quaternary chalcogenides, Adv. Funct. Mater. 32 (32) (2022), 2202157.

[8] Z. Bu, X. Zhang, Y. Hu, Z. Chen, S. Lin, W. Li, C. Xiao, Y. Pei, A record thermoelectric efficiency in tellurium-free modules for low-grade waste heat recovery, Nat. Commun. 13 (1) (2022) 237.

[9] L.-D. Zhao, J. He, D. Berardan, Y. Lin, J.-F. Li, C.-W. Nan, N. Dragoe, BiCuSeO oxyselenides: new promising thermoelectric materials, Energy Environ. Sci. 7 (9) (2014) 2900–2924.

[10] K. Guo, Y. Zhang, S. Yuan, Q. Tang, C. Lin, P. Luo, J. Yang, S. Pan, L.-D. Zhao, G. Cheng, J. Zhang, J. Luo, NaCdSb: an orthorhombic zintl phase with exceptional intrinsic thermoelectric performance, Angew. Chem. Int. Ed. 62 (3) (2023), e202212515.

[11] H. Zhu, J. Mao, Y. Li, J. Sun, Y. Wang, Q. Zhu, G. Li, Q. Song, J. Zhou, Y. Fu, R. He, T. Tong, Z. Liu, W. Ren, L. You, Z. Wang, J. Luo, A. Sotnikov, J. Bao, K. Nielsch, G. Chen, D.J. Singh, Z. Ren, Discovery of TaFeSb-based half-Heuslers with high thermoelectric performance, Nat. Commun. 10 (1) (2019) 270.

[12] Z. Liu, Q. Zhang, U. Wolff, C.G.F. Blum, R. He, A. Bahrami, M. Beier-Ardizzon, C. Reimann, J. Friedrich, H. Reith, G. Schierning, K. Nielsch, High-performance n-type Ge-free silicon thermoelectric material from silicon waste, ACS Appl. Mater. Interfaces 13 (40) (2021) 47912–47920.

[13] A.J. Minnich, M.S. Dresselhaus, Z.F. Ren, G. Chen, Bulk nanostructured thermoelectric materials: current research and future prospects, Energy Environ. Sci. 2 (5) (2009) 466–479.

[14] R. He, G. Schierning, K. Nielsch, Thermoelectric devices: a review of devices, architectures, and contact optimization, Advanced Materials Technologies 3 (4) (2018), 1700256.

[15] P. Ying, R. He, J. Mao, Q. Zhang, H. Reith, J. Sui, Z. Ren, K. Nielsch, G. Schierning, Towards tellurium-free thermoelectric modules for power generation from low-grade heat, Nat. Commun. 12 (1) (2021) 1121.

[16] M.S. Dresselhaus, G. Chen, M.Y. Tang, R.G. Yang, H. Lee, D.Z. Wang, Z.F. Ren, J.-P. Fleurial, P. Gogna, New directions for low-dimensional thermoelectric materials, Adv. Mater. 19 (8) (2007) 1043–1053.

[17] R. Venkatasubramanian, E. Siivola, T. Colpitts, B. O'Quinn, Thin-film thermoelectric devices with high room-temperature figures of merit, Nature 413 (6856) (2001) 597–602.

[18] J.-F. Li, W.-S. Liu, L.-D. Zhao, M. Zhou, High-performance nanostructured thermoelectric materials, NPG Asia Mater. 2 (4) (2010) 152–158.

[19] R. Mulla, A.O. White, C.W. Dunnill, A.R. Barron, The role of graphene in new thermoelectric materials, Energy Adv. (2023), https://doi.org/10.1039/D3YA00085K.

[20] H. Mun, S.-M. Choi, K.H. Lee, S.W. Kim, Boundary engineering for the thermoelectric performance of bulk alloys based on bismuth telluride, ChemSusChem 8 (14) (2015) 2312–2326.

[21] S. Ohno, U. Aydemir, M. Amsler, J.-H. Pöhls, S. Chanakian, A. Zevalkink, M. A. White, S.K. Bux, C. Wolverton, G.J. Snyder, Achieving zT > 1 in inexpensive zintl phase Ca9Zn4+xSb9 by phase boundary mapping, Adv. Funct. Mater. 27 (20) (2017), 1606361.

[22] R. Mulla, M.H.K. Rabinal, Copper sulfides: earth-abundant and low-cost thermoelectric materials, Energy Technol. 7 (7) (2019), 1800850.

[23] P. Ying, H. Reith, K. Nielsch, R. He, Geometrical optimization and thermal-stability characterization of Te-free thermoelectric modules based on MgAgSb/Mg3(Bi,Sb)2, Small 18 (24) (2022), 2201183.

[24] Z.-H. Ge, L.-D. Zhao, D. Wu, X. Liu, B.-P. Zhang, J.-F. Li, J. He, Low-cost, abundant binary sulfides as promising thermoelectric materials, Mater. Today 19 (4) (2016) 227–239.

[25] G. Dennler, R. Chmielowski, S. Jacob, F. Capet, P. Roussel, S. Zastrow, K. Nielsch, I. Opahle, G.K.H. Madsen, Are binary copper sulfides/selenides really new and promising thermoelectric materials? Adv. Energy Mater. 4 (9) (2014), 1301581.

[26] R. Mulla, D.R. Jones, C.W. Dunnill, Economical and facile route to produce gram-scale and phase-selective copper sulfides for thermoelectric applications, ACS Sustain. Chem. Eng. 8 (37) (2020) 14234–14242.

[27] L.-D. Zhao, S.-H. Lo, J. He, H. Li, K. Biswas, J. Androulakis, C.-I. Wu, T.P. Hogan, D.-Y. Chung, V.P. Dravid, M.G. Kanatzidis, High performance thermoelectrics from earth-abundant materials: enhanced figure of merit in PbS by second phase nanostructures, J. Am. Chem. Soc. 133 (50) (2011) 20476–20487.

[28] S. Zhan, T. Hong, B. Qin, Y. Zhu, X. Feng, L. Su, H. Shi, H. Liang, Q. Zhang, X. Gao, Z.-H. Ge, L. Zheng, D. Wang, L.-D. Zhao, Realizing high-ranged thermoelectric performance in PbSnS2 crystals, Nat. Commun. 13 (1) (2022) 5937.

[29] S. Bayesteh, S. Sailler, H. Schlörb, R. He, G. Schierning, K. Nielsch, N. Pérez, Mobility-enhanced thermoelectric performance in textured nanograin Bi2Se3, effect on scattering and surface-like transport, Materials Today Physics 24 (2022), 100669.

[30] Z.-H. Ge, P. Qin, D. He, X. Chong, D. Feng, Y.-H. Ji, J. Feng, J. He, Highly enhanced thermoelectric properties of Bi/Bi2S3 nanocomposites, ACS Appl. Mater. Interfaces 9 (5) (2017) 4828–4834.

[31] J. Recatala-Gomez, H.K. Ng, P. Kumar, A. Suwardi, M. Zheng, M. Asbahi, S. Tripathy, I. Nandhakumar, M.S.M. Saifullah, K. Hippalgaonkar, Thermoelectric properties of substoichiometric electron beam patterned bismuth sulfide, ACS Appl. Mater. Interfaces 12 (30) (2020) 33647–33655.

[32] Y. Wu, Q. Lou, Y. Qiu, J. Guo, Z.-Y. Mei, X. Xu, J. Feng, J. He, Z.-H. Ge, Highly enhanced thermoelectric properties of nanostructured Bi2S3 bulk materials via carrier modification and multi-scale phonon scattering, Inorg. Chem. Front. 6 (6) (2019) 1374–1381.

[33] D. Cadavid, M. Ibáñez, U. Anselmi-Tamburini, O.J. Durá, M.A.L.d.l. Torre, A. Cabot, Thermoelectric properties of bottom-up assembled Bi 2 S 3– x Te x nanocomposites, 9–1011, Int. J. Nanotechnol. 11 (2014) 773–784.

[34] Z.-H. Ge, B.-P. Zhang, Y.-Q. Yu, P.-P. Shang, Fabrication and properties of Bi2−xAg3xS3 thermoelectric polycrystals, J. Alloys Compd. 514 (2012) 205–209.

[35] Z.-H. Ge, B.-P. Zhang, J.-F. Li, Microstructure composite-like Bi2S3 polycrystals with enhanced thermoelectric properties, J. Mater. Chem. 22 (34) (2012) 17589–17594.

[36] Z.-H. Ge, B.-P. Zhang, P.-P. Shang, J.-F. Li, Control of anisotropic electrical transport property of Bi2S3 thermoelectric polycrystals, J. Mater. Chem. 21 (25) (2011) 9194–9200.

[37] W. Liu, C.F. Guo, M. Yao, Y. Lan, H. Zhang, Q. Zhang, S. Chen, C.P. Opeil, Z. Ren, Bi2S3 nanonetwork as precursor for improved thermoelectric performance, Nano Energy 4 (2014) 113–122.

[38] R. Mulla, K. Glover, C.W. Dunnill, An easily constructed and inexpensive tool to evaluate the Seebeck coefficient, IEEE Trans. Instrum. Meas. 70 (2021) 1–7.

[39] R. Mulla, M.K. Rabinal, A simple and portable setup for thermopower measurements, ACS Comb. Sci. 18 (4) (2016) 177–181.

[40] B.M. Zawilski, R.T.L. IV, T.M. Tritt, Description of the parallel thermal conductance technique for the measurement of the thermal conductivity of small diameter samples, Rev. Sci. Instrum. 72 (3) (2001) 1770–1774.

[41] R. Mulla, C.W. Dunnill, Core–shell nanostructures for better thermoelectrics, Materials Advances 3 (1) (2022) 125–141.

[42] A. Pakdel, Q. Guo, V. Nicolosi, T. Mori, Enhanced thermoelectric performance of Bi–Sb–Te/Sb2O3 nanocomposites by energy filtering effect, J. Mater. Chem. 6 (43) (2018) 21341–21349.

[43] P.P. Murmu, V. Karthik, Z. Liu, V. Jovic, T. Mori, W.L. Yang, K.E. Smith, J. V. Kennedy, Influence of carrier density and energy barrier scattering on a high Seebeck coefficient and power factor in transparent thermoelectric copper iodide, ACS Appl. Energy Mater. 3 (10) (2020) 10037–10044.